Original Article

Genetic differences between lung metastases and liver metastases from left-sided microsatellite stable colorectal cancer: next generation sequencing and clinical implications

Zhenghang Wang[1], Xue Zheng[2], Xicheng Wang[1], Yawei Chen[2], Zhongwu Li[3], Jianing Yu[2], Wanning Yang[2], Beibei Mao[2], Henghui Zhang[2,4], Jian Li[1], Lin Shen[1]

[1]Department of Gastrointestinal Oncology, Key Laboratory of Carcinogenesis and Translational Research (Ministry of Education), Peking University Cancer Hospital & Institute, Beijing, China; [2]Genecast Biotechnology Co., Ltd., Wuxi, China; [3]Department of Pathology, Key Laboratory of Carcinogenesis and Translational Research (Ministry of Education), Peking University Cancer Hospital & Institute, Beijing, China; [4]Institute of Infectious Diseases, Beijing Ditan Hospital, Capital Medical University, Beijing Key Laboratory of Emerging Infectious Diseases, Beijing, China

Contributions: (I) Conception and design: Z Wang, X Zheng; (II) Administrative support: L Shen, J Li; (III) Provision of study materials or patients: X Zheng, X Wang, Y Chen, Z Li; (IV) Collection and assembly of data: Z Wang, J Yu, W Yang, B Mao, H Zhang; (V) Data analysis and interpretation: All authors; (VI) Manuscript writing: All authors; (VII) Final approval of manuscript: All authors.

Correspondence to: Lin Shen, PhD, MD. Key Laboratory of Carcinogenesis and Translational Research (Ministry of Education), Peking University Cancer Hospital & Institute, Fucheng Road No. 52, Haidian District, Beijing, China. Email: shenlin@bjmu.edu.cn; Jian Li, PhD, MD. Key Laboratory of Carcinogenesis and Translational Research (Ministry of Education), Peking University Cancer Hospital & Institute, Fucheng Road No. 52, Haidian District, Beijing, China. Email: oncogene@163.com.

Background: Data regarding the clinical characteristics and outcomes of lung metastases (LuM) from colorectal cancer (CRC) are different from those of liver metastases (LiM) from CRC. However, little is known about the genetic features of LuM. This study aimed to identify the different genetic characteristics of LuM and LiM from left-sided microsatellite stable CRC.

Methods: Tissue samples of the primary tumors and paired metastases from 18 CRC patients with isolated LuM (LuM cohort), 18 patients with isolated LiM (LiM cohort), and 10 locally advanced CRC patients without metastases (control cohort) were selected for next-generation sequencing. Patients in the LiM cohort had matched clinicopathological characteristics with the LuM cohort. The single-nucleotide variations (SNVs), copy number variations (CNVs), pathway alterations, and tumor mutation burdens (TMBs) were also calculated and analyzed.

Results: The CNV results showed that *ZFHX4*, *GATA2*, and *FAM131B* amplifications were more common in the metastatic cohorts than in the control cohort, while *RECQL4* and *FLCN* amplifications were common in the controls. The LuM cohort had significantly higher proportions of *HNF4A*, *BRD4*, and *U2AF1* amplification. The LuM, LiM, and control cohorts were successfully separated using pathway alteration analysis. The LuM cohort had more frequent alterations in the RTK/RAS pathway, HIPPO pathway, *KRAS*, and *MET* than the LiM group. The LuM cohort also had relatively higher TMBs than the LiM cohort.

Conclusions: CNVs in primary tumors could identify patients with LuM. Targeting the HIPPO pathway or *MET* and immune checkpoint inhibitors (ICIs) combined with other agents might be novel therapies for LuM.

Keywords: colorectal cancer (CRC); lung metastasis; liver metastasis; copy number variation (CNV); tumor mutation burden (TMB)

Submitted Mar 22, 2021. Accepted for publication Jun 15, 2021.
doi: 10.21037/atm-21-2221
View this article at: https://dx.doi.org/10.21037/atm-21-2221

Introduction

Colorectal cancer (CRC) ranks as the third most commonly occurring cancer worldwide (1), while metastasis is the major cause of death in patients with cancer. The liver is one of the most frequent sites in which malignancies preferentially metastasize, followed by the lungs, lymph nodes, bone, and brain. Rectal cancers, especially middle and lower rectal cancers, tend to metastasize to the lungs and bones. While colon cancers mainly have a higher incidence of liver metastases (LiM) (2). Given that China has a much higher incidence of rectal cancer than Western countries (3), treating CRC patients with lung metastases (LuM) is also an urgent health issue.

Patients with resected LiM could benefit from radical resection with perioperative treatments. However, most patients had unresectable LiM and should receive palliative pharmacotherapy as the standard care. It is currently recommended to apply the therapeutic strategy of LiM for patients with LuM due to the lack of specific guidelines for managing LuM CRC. Approximately only 10% of patients with initial LuM can undergo radical resection (4,5) but they do not receive any benefits from adjuvant chemotherapy (6). Compared with LiM (7,8), the possibility of conversion from unresectable LuM to resectable LuM is relatively low (5.7–7.1%) (5). Therefore, the standard treatment for most patients with LuM or LiM is pharmacotherapy, including chemotherapy and targeted agents. However, many metastatic CRC patients who failed to respond to standard therapies still have good Karnofsky performance status, yet no other drugs are available for use. This phenomenon is more obvious in CRC with LuM, since patients with LuM have longer survival duration and slower growth of cancer cells compared to LiM (9). The acquisition of the tumor genetic profiles may screen out specific targets of LuM. For instance, the frequency of HER2 positivity in LuM is 4%, which is significantly higher than that in the primary tumor (1.8%) (10). In the HERACLES and MyPathway trials, the promising antitumor activity of dual anti-HER2 therapy was observed (11,12), indicating that HER2 might be a valuable therapeutic target of LuM.

Limited data of the genetic features of LuM have been reported. A small case-match study has revealed that de novo mutations in LuM are different from those in LiM (13). A previous study has also demonstrated that *KRAS* and *PIK3CA* mutations are associated with the development of LuM (14). Taken together, the above evidence suggests that LuM may represent a unique molecular subtype from that of LiM in CRC patients. However, current findings are far from enough for a full elucidation of the genetic features of LuM compared to LiM. More biomarkers and targets are still needed in clinical practice. Therefore, this pilot study aimed to provide novel insights of genetic differences between LuM and LiM.

Some clinical and pathological characteristics, such as primary tumor location (left *vs.* right) and microsatellite instability (MSI) status (microsatellite stability *vs.* MSI), are associated with genetic profiles of metastatic CRC (15). This study focused on microsatellite stable (MSS) left-sided CRC which represented the most cases of CRC. To reduce other potential confounding factors that might influence the genetic features, we selected patients with isolated LuM, and matched them with isolated LiM patients according to the clinicopathological features, including age, sex, primary location, T stage, N stage, histology, and differentiation grade. As a result, the different genetic profiles between the LuM and LiM cohorts in this study could be considered as true molecular differences, while previous studies of genetic profiles in CRC did not establish these well-matched cohorts. By comparing the genetic profiles of primary tumors and the corresponding metastases from patients with LuM and LiM using next-generation sequencing (NGS), we found that the CNV characteristics of primary tumors can be used as a marker to distinguish LuM patients from LiM patients and patients without metastasis. The LuM cohort had more frequent alterations in the RTK/RAS pathway, HIPPO pathway, *KRAS* and *MET* than the LiM group. We present the following article in accordance with the MDAR reporting checklist (available at https://dx.doi.org/10.21037/atm-21-2221).

Methods

Patients

The clinical data of 213 patients with isolated LuM CRC who received treatment between 2008 and 2016 were retrospectively reviewed at the Department of Gastrointestinal Oncology, Peking University Cancer Hospital & Institute. The main inclusion criteria of the LuM cohort were as follows: (I) had a biopsy or surgery of both the primary tumor and LuM; (II) both primary tumor and LuM tissue samples were available; (III) patients were diagnosed with left-sided CRC with isolated LuM. After excluding unqualified participants, a total of 18 LuM CRC patients were included in the LuM cohort.

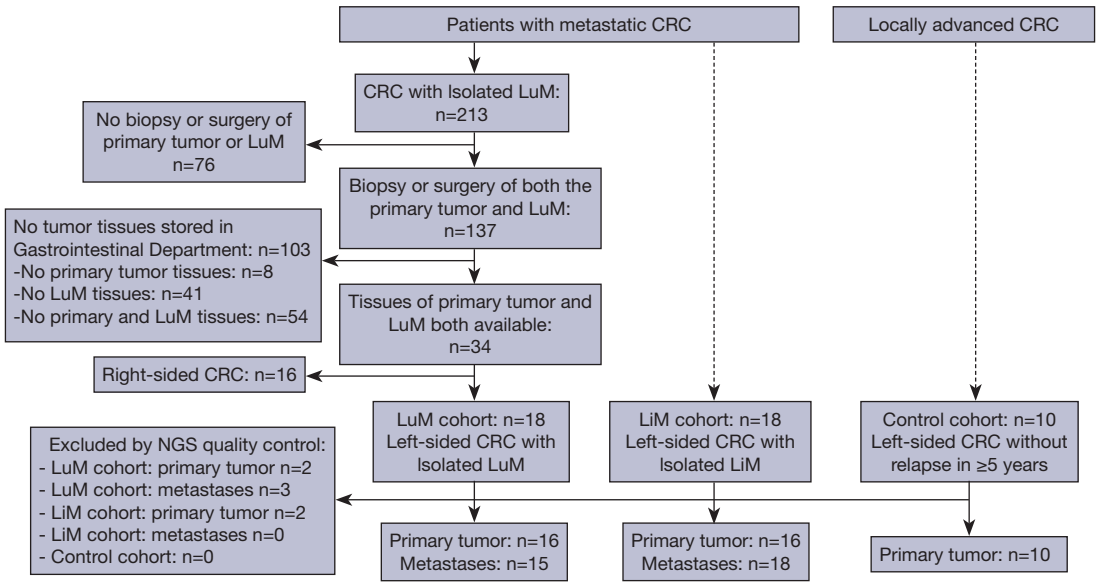

Figure 1 Flow diagram of patient selection. The LiM and LuM cohorts were matched 1:1 according to age (within the range of ±10 years, with the LuM patient as the reference), sex (male, female), primary location (left colon, upper rectum, middle rectum, and lower rectum), T stage (T1–2, T3–4), N stage (positive, negative), histology (with or without a mucinous carcinoma or signet ring cell carcinoma component), and differentiation grade (well to moderate, poor to undifferentiated). CRC, colorectal cancer; LuM, lung metastases; LiM, liver metastases; NGS, next-generation sequencing.

To investigate the different genetic characteristics between LuM and LiM, we also selected 18 patients with left-sided CRC with isolated LiM as the LiM cohort. The patients in the LiM cohort had matched clinicopathological characteristics as the LuM cohort to minimize bias in the study, including age, sex, primary location, T stage, N stage, histology, and differentiation grade. In addition, 10 patients with locally advanced CRC who underwent radical surgery without relapse within the last 5 years were also selected as the control cohort. The small sample size in the control cohort was due to the limited number of patients with locally advanced CRC admitted to our department. The detailed selection process is demonstrated in *Figure 1*. This study was conducted in accordance with the Declaration of Helsinki (as revised in 2013). This study was approved by the Beijing Cancer Hospital Ethics Committee (No. 2017KT91) and individual consent for this retrospective analysis was waived.

Tissue samples

Tissue samples from the LuM (n=18) cohort, the LiM (n=18) cohort, and the control cohort (n=10) were collected. Each sample had been stored for 2–5 years prior to the study. In the metastatic cohorts (LuM and LiM cohorts), 23 out of the 36 primary tumor tissues had pre-operative treatment, while the other 13 had upfront resection after being diagnosed. Four of the 18 LuM tissue samples received pre-operative treatment, whereas 17 of the 18 LiM tissue samples had pre-operative treatment. All of the tissue samples from the control cohort received upfront resection.

DNA extraction

Genomic DNA was extracted from formalin-fixed paraffin-embedded (FFPE) tumor tissues and fresh tissues soaked in preservation solution using a blackPREP FFPE DNA Kit (Analytik Jena, Germany) and a Tiangen Genomic DNA Kit (Tiangen, Beijing, PRC), respectively. The DNA concentration was measured using a Qubit dsDNA HS Assay Kit (Life Technologies, California, USA) following the manufacturer's protocol. The extracted DNA was stored at –20 ℃ or directly interrupted.

Targeted sequencing

Genomic DNA was sheared into 150–200 bp fragments using a Covaris M220 Focused-ultrasonicator (Covaris,

Massachusetts, USA). Once the fragment size met the requirements, the KAPA HTP Library Preparation Kit (Illumina platform, KAPA Biosystems, Massachusetts, USA) was applied to construct the DNA Library according to the manufacturer's instructions. The DNA library was captured with a designed 1406-gene panel (Genecast, Beijing, China) that included major tumor-related genes. The captured samples were then subjected to a HiSeq X-Ten system (Illumina, San Diego, California, USA) for paired-end sequencing.

Variant calling of single-nucleotide variations (SNVs) and insertions and deletions (indels)

We used the Mutect2 tool from the Genome Analysis Toolkit (GATK v3.7) to collect somatic SNVs as well as insertions and deletions (indel) in tumor and normal samples. The NimbleDesign assay (1,406 genes) was used to identify mutations. The following filters were applied: (I) for mutations that were not in COSMIC (https://cancer.sanger.ac.uk/cosmic): mutant allele frequency >3% and tumor variant frequency 5 times higher than normal tissue; for mutations in COSMIC and passed the Mutect2 filter: mutant allele frequency >1% and tumor variant frequency 5 times higher than normal tissues; for mutations in COSMIC but did not pass the Mutect2 filter: mutant allele frequency >1% and tumor variant frequency 10 times higher than normal tissues; (II) the number of mutant allele reads >5; (III) coverage >50; (IV) allele frequency <20% using a group of healthy human plasma samples from the Genecast database (n=30); (V) nonsynonymous SNVs and indels; (VI) located in exon regions; and (VII) allele frequency <0.5% in the Exosome Aggregation Consortium (ExAC) (http://exac.broadinstitute.org) and allele frequency <1% in the 1,000 Genomes Project (http://www.internationalgenome.org/data/).

Calling of copy number variations (CNVs)

We used the CNVkit (v0.9.2) to obtain the $\log_2$ copy ratio from the tumor samples of each patient and each gene. A panel of healthy control blood samples was used for reference construction. A gene was defined as copy number gain ($\log_2$ copy ratio $<\log_2 1.5$) or loss ($\log_2$ copy ratio $<-\log_2 5/3$) when the number of target intervals was ≥5.

Tumor mutation burden (TMB) calculation

For the determination of TMB, the number of somatic nonsynonymous SNVs (with depth >100× and allele frequency ≥2%) detected with NGS (interrogating Mb of the genome) was quantified, and the value was extrapolated to the whole exome. Targeted sequencing was performed for TMB calculation. Alterations which are known to be bona fide oncogenic drivers were excluded. TMB was measured in mutations per Mb.

Hierarchical clustering and pathway alteration analysis

We performed hierarchical clustering based on Euclidean distance using the heatmap package in R software. The corresponding gene mutations were extracted and the gene landscape was obtained using specific pathways, as described in previous research (15).

Statistical analyses

Statistical analyses were performed using R version 3.6.0, SPSS version 19.0 (SPSS, Inc., Chicago, IL, USA), and GraphPad Prism (version 7.00, La Jolla, CA, USA) software. Differences between proportions were evaluated using Fisher's exact test. The Kruskal-Wallis test was also applied to compare differences between multiple groups, while Dunn's multiple comparisons test was carried out to compare differences between 2 groups. All of the tests were two-sided, and P values less than 0.05 were regarded as statistically significant.

Results

Clinicopathological characteristics

A total of 46 participants were involved in this study, including 18 in the LuM cohort, 18 in the LiM cohort, and 10 in the control cohort. Two of the 18 primary tumors and 3 of the 18 metastatic lesions in the LuM cohort, and 2 of the 18 primary tumors in the LiM cohort failed to pass the quality control for NGS, and were therefore excluded from further genetic analysis. The clinicopathological characteristics of each cohort were collected and analyzed (*Table 1*). Approximately 60% of patients were male. The most common primary location of tumors was the rectum. The T stage was T3–4 in all cases, while the N stage was

Table 1 Clinicopathological characteristics of the whole population and the population involved in the final analysis

Characteristics	LuM cohort, n (%)			LiM cohort, n (%)			Control cohort, n (%)	P
	Total (n=18)	Analyzed		Total (n=18)	Analyzed		Total/analyzed (n=10)	
		Primary (n=16)	Metastases (n=15)		Primary (n=16)	Metastases (n=18)		
Sex								1.000
Male	11 (61.1)	9 (56.3)	10 (66.7)	11 (61.1)	9 (56.3)	11 (61.1)	6 (60.0)	
Female	7 (38.9)	7 (43.8)	5 (33.3)	7 (38.9)	7 (43.8)	7 (38.9)	4 (40.0)	
Age (years)								0.661
Median (range)	57.5 (35-79)	57.5 (35-79)	56 (35-79)	58 (38-74)	58 (42-74)	58 (38-74)	57 (42-69)	
≤60	12 (66.7)	11 (68.8)	10 (66.7)	11 (61.1)	10 (62.5)	11 (61.1)	8 (80.0)	
>60	6 (33.3)	5 (31.3)	5 (33.3)	7 (38.9)	6 (37.5)	7 (38.9)	2 (20.0)	
Primary location								0.124
Left colon	2 (11.1)	2 (12.5)	2 (13.3)	2 (11.1)	2 (12.5)	2 (11.1)	4 (40.0)	
Rectum	16 (88.9)	14 (87.5)	13 (86.7)	16 (88.9)	14 (87.5)	16 (88.9)	6 (60.0)	
T stage								N/A
T1–2	0 (0.0)	0 (0.0)	0 (0.0)	0 (0.0)	0 (0.0)	0 (0.0)	0 (0.0)	
T3–4	18 (100.0)	16 (100.0)	15 (100.0)	18 (100.0)	16 (100.0)	18 (100.0)	10 (100.0)	
N stage								0.491
N0	2 (11.1)	2 (12.5)	2 (13.3)	2 (11.1)	2 (12.5)	2 (11.1)	3 (30.0)	
N1–2	16 (88.9)	14 (87.5)	13 (86.7)	16 (88.9)	14 (87.5)	16 (88.9)	7 (70.0)	
Histopathologic type								1.000
Adenocarcinoma	17 (94.4)	16 (100.0)	14 (93.3)	17 (94.4)	15 (93.8)	17 (94.4)	10 (100.0)	
Mucinous carcinoma/signet ring cell carcinoma ± adenocarcinoma	1 (5.6)	0 (0.0)	1 (6.7)	1 (5.6)	1 (6.3)	1 (5.6)	0 (0.0)	
Differentiation grade								0.823
Well to moderate	14 (77.8)	14 (87.5)	11 (73.3)	14 (77.8)	12 (75.0)	14 (77.8)	7 (70.0)	
Poor to undifferentiated	4 (22.2)	2 (12.5)	4 (26.7)	4 (22.2)	4 (25.0)	4 (22.2)	3 (30.0)	

LuM, lung metastases; LiM, liver metastases; AMP, amplification.

positive in most cases.

Genetic landscapes of the primary tumors

All primary tumors were MSS. The most common mutated gene was *TP53* (69%), followed by *APC* (64%) and *KRAS* (31%) in the whole population. No significant difference in SNVs was observed between the metastatic (LuM + LiM) cohort and the control cohort or between the LuM and LiM cohorts (*Figure 2A*, Table S1).

The results of CNVs showed that *ZFHX4* (90.6% *vs.* 10.0%, P<0.001), *GATA2* (34.4% *vs.* 0.0%, P=0.081), and *FAM131B* (34.4% *vs.* 0.0%, P=0.081) were commonly amplified in the metastatic cohort compared to the control cohort, while *RECQL4* (6.3% *vs.* 70.0%, P<0.001) and *FLCN* (0.0% *vs.* 30.0%, P=0.010) were commonly amplified in the control cohort (*Figure 2B*, Table S2). Based on the CNV data of the 5 selected genes (*FLCN*, *RECQL4*, *ZFHX4*, *GATA2*, and *FAM131B*), hierarchical clustering of all the primary tumors revealed that the metastatic cohort and control cohort formed 2 separate clusters (*Figure 2C*).

The LuM cohort had significantly higher proportions of *HNF4A* (43.8% *vs.* 0.0%, P=0.007), *BRD4* (50.0% *vs.* 6.3%, P=0.015), and *U2AF1* (31.3% *vs.* 0.0%, P=0.043) amplification than those in the LiM cohort (*Figure 2B*, Table S2). Based on the CNVs of 3 selected genes (*HNF4A*, *BRD4*, and *U2AF1*) (P<0.05), hierarchical clustering of the primary tumors from the metastatic cohort demonstrated that 13 of the LuM patients and 2 of the LiM patients formed a cluster, while the remaining patients (3 LuM patients and 14 LiM patients) formed another cluster (*Figure 2D*).

As patients with middle or lower rectal cancer are more likely to develop LuM than those with upper rectal cancer or left-sided colon cancer because of venous drainage (16), we further classified patients into a 'middle/lower rectum' group and a 'colon/upper rectum' group. The results indicated that the differences in gene amplification between the LuM and LiM cohorts in the middle/lower rectum group were comparable to those in the colon/upper rectum group (Figure S1).

Pathway alteration analysis

The landscapes of 10 selected pathways and their frequencies, including WNT, TGFβ, RTK/RAS, PI3K, P53, NRF2, NOTCH, MYC, HIPPO, and cell cycle, in the primary and metastatic lesions of all cohorts are demonstrated in *Figure 3* and Table S3. In all of the specimens involving primary and metastatic tumors, the 3 most altered pathways were RTK/RAS (80.0%), P53 (76.0%), and WNT (68.0%), while the alteration frequency of the other pathways ranged from 2.6% (the NRF2 pathway) to 42.1% (the NOTCH pathway).

The analysis of pathway alterations in the primary tumors showed that the LuM cohort had a higher rate (87.5%) of RTK/RAS pathway alterations than the LiM (68.8%) and control (70%) cohorts, with no significant differences. PI3K pathway alterations were more common (50.0%) in the LuM cohort with no statistical significance. The rest of the pathways had similar alterations in the 3 cohorts (*Figure 3*, Table S3).

Regarding metastatic tumors, LuM was significantly associated with RTK/RAS pathway alterations (100% *vs.* 72.2%, P=0.049) compared with LiM. Furthermore, the P53 pathway (93.3% *vs.* 66.7%, P=0.095) and the HIPPO pathway (33.3% *vs.* 5.6%, P=0.070) showed more frequent alterations in the LuM cohort than in the LiM cohort (*Figure 3*, Table S3).

In the RTK/RAS pathway of the LuM cohort, the alteration frequency of *KRAS* was the most common (73.3%) one, which was markedly higher than that in the LiM cohort (38.9%, P=0.080). In the primary tumors of the LuM cohort, the *KRAS* alteration frequency was 43.8%, which was slightly higher than the LiM (31.3%) and control (30.0%) cohorts. The *MET* alteration rate was 40.0% and 5.6% in LuM and LiM, respectively (P=0.030), whereas there were no *MET* alterations in the primary tumors (*Figure 3*).

Genetic characteristics associated with immune checkpoint inhibitors (ICIs)

The median TMB of the primary tumors in the LuM cohort was 9.518 SNVs/Mb, which was significantly higher than that in the LiM (1.003 SNVs/Mb, P=0.003) and control (3.987 SNVs/Mb, P=0.030) cohorts. Meanwhile, the LuM cohort demonstrated notably higher TMB levels than the LiM cohort (6.022 *vs.* 2.02 SNVs/Mb, P=0.044) (*Figure 4*, *Table 2*). A TMB >10 SNVs/Mb was observed more frequently in samples from the LuM cohort than the other 2 cohorts (P=0.004) (*Table 2*).

The panel used in this study contained several genes whose alterations might contribute to the response (positive gene) or resistance (negative gene) to ICIs. The alteration frequencies of these positive and negative genes were not different between the primary and metastatic lesions or between different cohorts (*Figure 5*, Table S4).

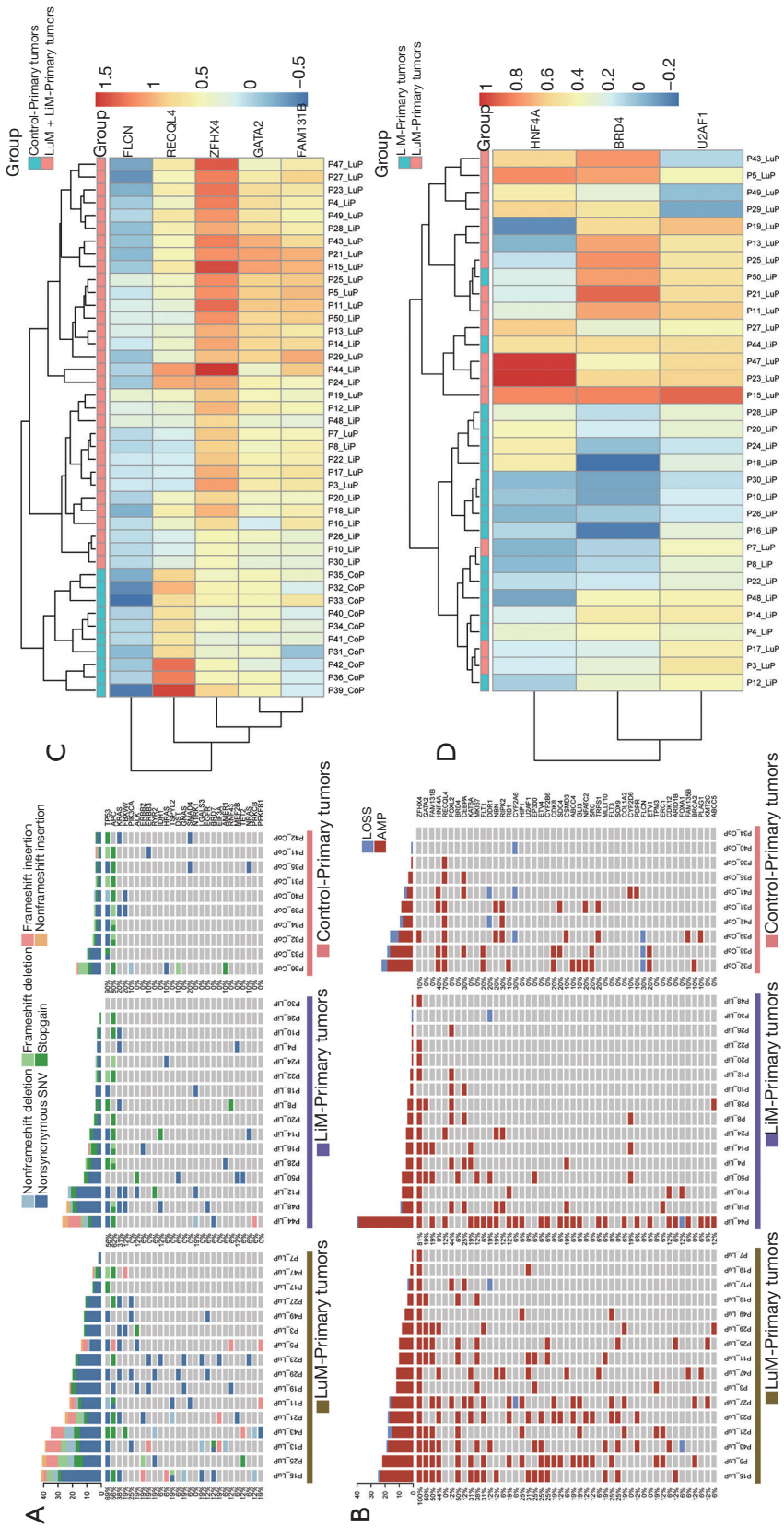

Figure 2 Genetic analysis of primary tumors from the LuM, LiM, and control cohorts. (A,B) Heatmap of single-nucleotide variations (A) and copy number variations (B) in the primary tumors (only the genes with a total population frequency of more than 5% are displayed). The alteration frequencies of each gene are listed on the left side of each cohort. (C,D) Heatmap of the log2 copy ratio profiles of the primary tumors. Hierarchical clustering analysis showed (C) perfect grouping of the control cohort (cyan) and the LuM + LiM cohorts (light coral) and (D) strong grouping of the LiM (cyan) and LuM (light coral) cohorts. Orange-red indicates that the copy number is greater than that of the healthy baseline; blue indicates that the copy number is less than that of the healthy baseline. LuM, lung metastases; LiM, liver metastases; AMP, amplification.

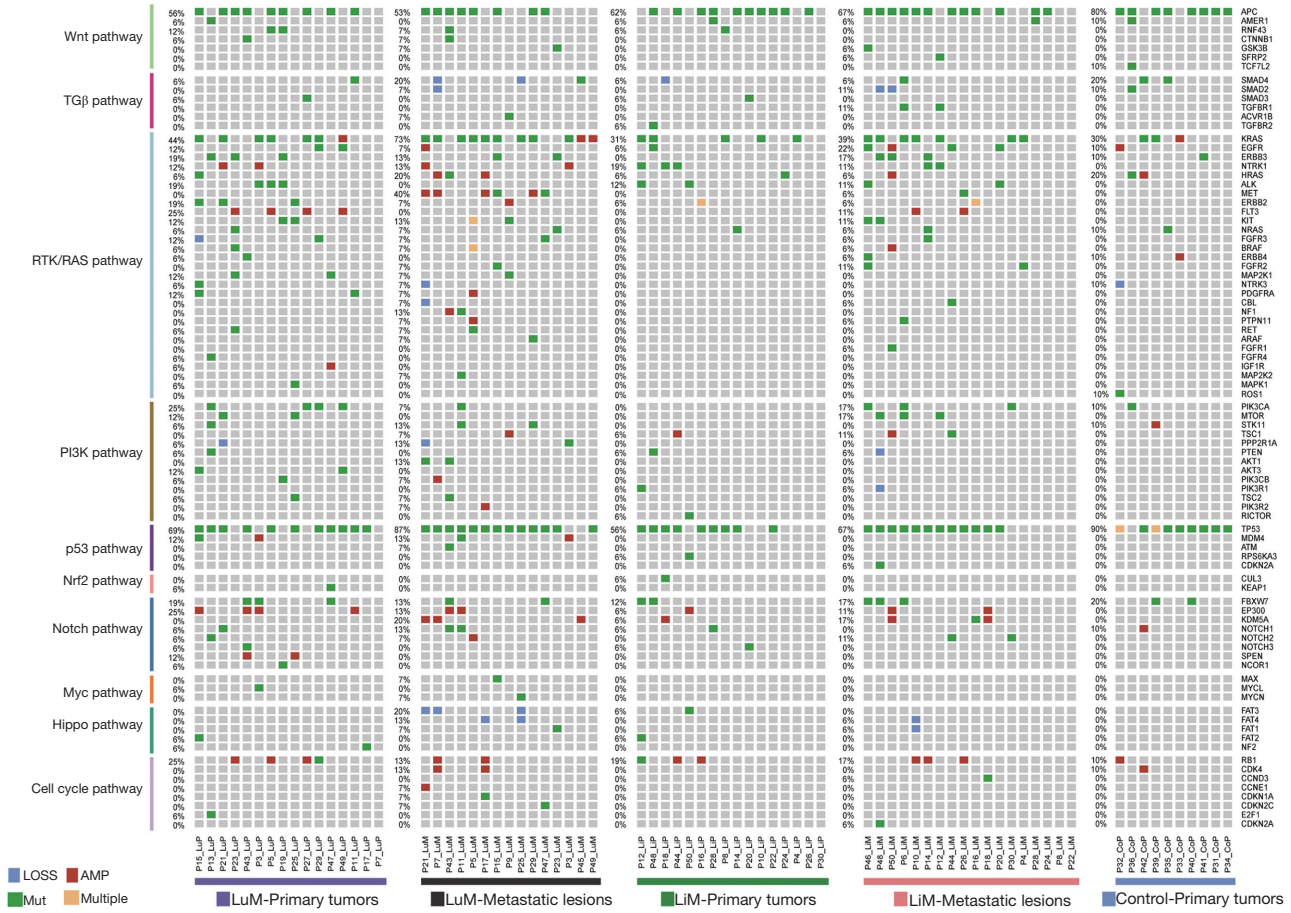

Figure 3 Alteration frequencies per gene in each pathway in the primary tumors and metastatic lesions. Blue: loss of copy number; red: AMP; green: SNV and/or indel; orange: concurrent variation (SNV, indel, or CNV). LuM, lung metastases; LiM, liver metastases; AMP, amplification; Mut, mutation; SNV, single-nucleotide variation; CNV, copy number variation.

Discussion

In this study, all primary tumors and metastatic lesions were MSS, indicating the high concordance of MSI status between primary tumors and metastases, which was in accordance with previous findings (17). Therefore, the population in this study was relatively homogeneous. Considering other clinical and pathological characteristics were also matched between LuM and LiM cohorts, it was believed that the different genetic profiles of LuM and LiM were relatively credible despite of the small sample number involved.

Early identification of locally advanced CRC patients who have a high risk of developing LuM can help with postoperative surveillance. Several clinical studies have shown that LuM is associated with *RAS* mutation (18-21), *PIK3CA* mutation (22), and *MTDH* amplification (23). However, the current findings regarding these gene alterations were not sufficient to predict LuM development. A previous study demonstrated that 45.3% of patients with *KRAS* mutations developed LuM, while 37.3% of patients developed LiM (19). Our results are consistent with the previous findings in that 13 patients had *KRAS* mutant primary tumors, 6 patients developed LuM, and 5 patients developed LiM. In 29 patients with *KRAS* wild-type primary tumors, 10 and 11 patients developed LuM and LiM, respectively.

We also compared the genetic profiles of primary tumors from the LuM cohort, the LiM cohort, and the control cohort to explore the 'metastatic signatures' of CRC using NGS. The results demonstrated that the amplifications of *ZFHX4*, *GATA2*, and *FAM31B* were common in the metastatic cohorts, while frequent amplifications of *FLCN*

and *RECQL4* were observed in the control cohort. Zinc Finger Homeobox 4 (ZFHX4), a putative transcription factor, plays a crucial role in regulating glioblastoma pathogenesis (24). In the CRC cell line HCT-116, which has high expression of ZFHX4, the cell-cell junctions become closer. In contrast, the down-regulation of ZFHX4 could inhibit the capacity for cell migration. Furthermore, patients with high *ZFHX4* mRNA levels are reported to have a poorer prognosis compared to those with low mRNA levels (25). GATA binding protein 2 (GATA2), a key member of the zinc finger transcription factor family, contributes to the development of hematopoietic malignant disorders and solid tumors, such as breast cancer and non-small cell lung cancer. High GATA2 expression is associated with later clinical stage of CRC (26). In our study, *GATA2* and *ZHFX4* were amplified more frequently in metastatic CRC than in locally advanced CRC, indicating that these genes might have important roles in tumor invasion and metastasis. Given that both *GATA2* and *ZHFX4* genes encode transcription factors, the regulation of transcription factors might be a potential metastatic mechanism of CRC by either activating oncogenes or inactivating suppressor genes. Further studies are required to validate the association of mRNA levels or protein expression with gene amplification, and to explore detailed metastatic mechanisms. RECQL4, one of the RECQ helicases, is responsible for unwinding double-stranded nucleic acids and maintaining genomic integrity. CRC patients had significantly higher mRNA levels of RECQL4 than normal colonic mucosa, which suggests the potential survival advantage of CRC cells over normal tissues (27). In our study, *RECQL4* amplification was detected in 7 out of 10 controls, while only 2 out of 32 metastatic patients had *RECQL4* amplification. We found that most primary tumors without metastases need *RECQL4* amplification to remain tumorigenic, while those with metastatic potential do not.

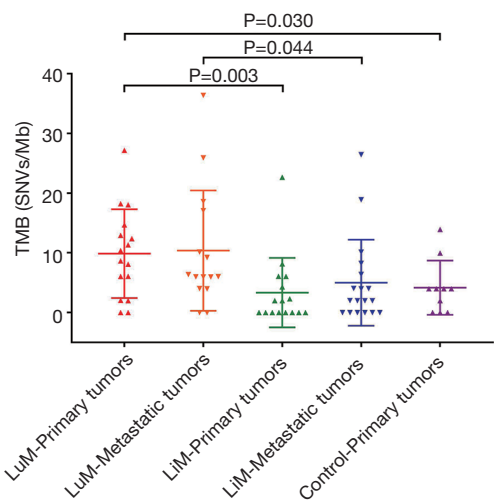

Figure 4 Tumor mutation burdens of the primary tumors and metastatic lesions. Data are mean ± SD. SNV, single-nucleotide variation; LuM, lung metastases; LiM, liver metastases; SD, standard deviation.

The results of hierarchical clustering analysis showed that patients with either LuM or LiM could be separated from those with locally advanced CRC in accordance with the CNVs of the above 5 genes, which raised the possibility of establishing a 'metastatic signature' of CRC.

Three additional genes, *BRD4*, *HNF4A*, and *U2AF1*, showed significantly higher amplification frequency in the LuM cohort than in the LiM cohort. *BRD4* is an epigenetic regulator that localizes to DNA by binding to acetylated histones and plays an important role in the pathogenesis of CRC (28,29). Preclinical work has demonstrated that *BRD4* inhibitors could inhibit tumor migration, invasion, and distal metastases (29). The transcription factor HNF4α, a member of the superfamily of nuclear receptors, has a pivotal role in oncogenic metabolism depending on the tissue specificity (30). The inhibition of tumor growth and proliferation in CRC after HNF4α suppression indicates that *HNF4A* is an oncogene (31). In the present study, *BRD4* and *HNF4A* amplification was observed in 50% and

Table 2 Tumor mutation burdens of primary and metastatic lesions in LuM, LiM and Control Cohorts

TMB (SNVs/Mb)	LuM cohort		LiM cohort		Control cohort	P
	Primary (n=16)	Metastases (n=15)	Primary (n=16)	Metastases (n=18)	Primary (n=10)	
Median	9.518	6.022	1.003	2.02	3.987	0.004
>10, n (%)	8 (50.0)	5 (33.3)	1 (6.3)	3 (16.7)	1 (10.0)	
>15, n (%)	3 (18.8)	4 (26.7)	1 (6.3)	2 (11.1)	0 (0.0)	

LuM, lung metastases; LiM, liver metastases.

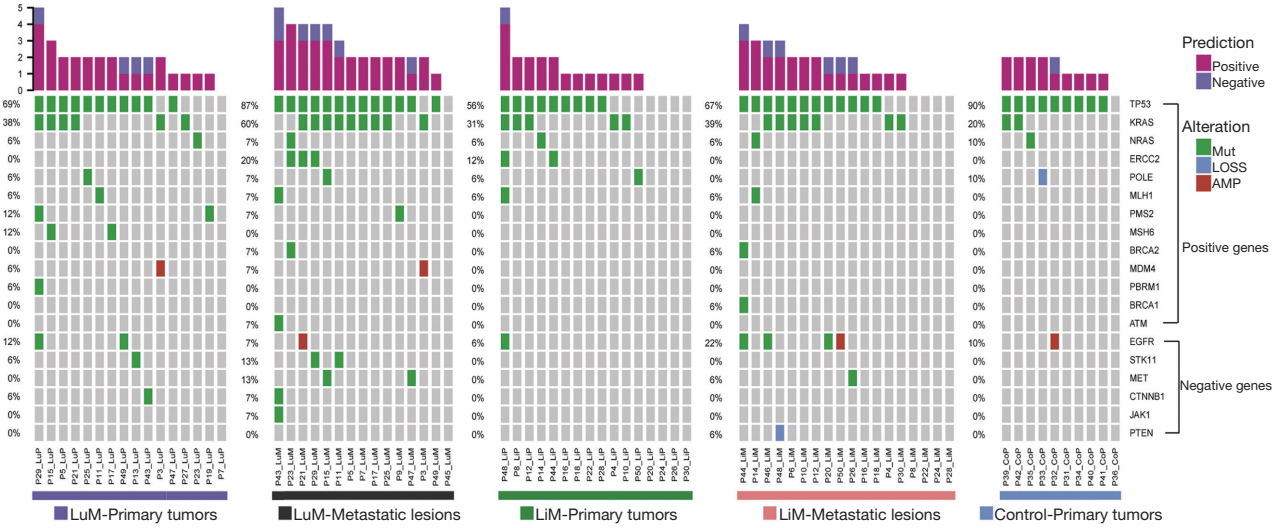

Figure 5 Gene alterations in the primary tumors and metastatic lesions probably associated with ICIs. "Positive" and "negative" genes indicate that the corresponding genes are associated with good and poor clinical outcomes, respectively, following treatment with ICIs. LuM, lung metastases; LiM, liver metastases; AMP, amplification; Mut, mutation; ICIs, immune checkpoint inhibitors.

43.8% of patients with LuM, respectively. Therefore, *BRD4* and *HNF4A* inhibitors may be able to reduce the risk of developing LuM.

Moreover, we found that 8 out of 9 patients with *BRD4* amplification, 7 patients with *HNF4A* amplification, and 5 patients with *U2AF1* amplification in the primary tumors developed LuM. Based on the CNV alterations specific to LuM, cases with LuM were separated from those with LiM in the hierarchical clustering. However, these findings should be further validated in an independent cohort with a large number of samples.

At present, pharmacotherapy is the major treatment strategy for metastatic tumors. Although LuM has better survival than most distal metastases (9), there are no effective drugs for patients with LuM. In this genetic analysis, we aimed to explore the possibility of new therapeutic targets and ICIs for patients with LuM. The comparison of pathway alterations between LuM and LiM demonstrated that the RTK/RAS pathway and *KRAS* alterations were enriched in the LuM cohort, indicating the ineffectiveness of anti-EGFR antibodies. Additionally, *MET* amplification and the activation of the HIPPO pathway which were common in LuM may serve as therapeutic targets for LuM.

The *MET* gene, an important oncogene, encodes the tyrosine kinase receptor for hepatocyte growth factor and promotes tumor growth, invasion, and metastasis (32). It is located upstream of the *KRAS* gene in the RTK/RAS pathway (15), while its amplification is an acquired mechanism of resistance to EGFR inhibitors (33). *MET* amplification was observed in approximately 1% of untreated metastatic CRC (mCRC) (33) and 1% of left-sided mCRC (34). Notably, none of the patients received anti-EGFR therapy in our LuM cohort, however, *MET* amplification was observed in 4 out of 16 (25%) LuM cases, indicating a potential role for *MET* inhibition in the therapeutic strategy of LuM.

In a multicenter phase 2 study, 41 anti-EGFR-resistant patients with high MET expression and wild-type *KRAS* mCRC received the MET inhibitor tivantinib plus cetuximab, which showed a 9.8% overall response rate (ORR) and 43.9% disease control rate. In 13 tested patients with *MET* amplification, 2 patients with *MET* amplification achieved partial response (PR), while only 1 of the 11 patients without *MET* amplification achieved PR (32). Therefore, anti-MET therapy might be suitable for MET-amplified LuM. Nevertheless, it should be noted that all cases of *MET* amplification in this study were accompanied by *KRAS* mutations (*Figure 3*). Consequently, the combination of *MET* inhibitors and *KRAS* inhibitors, such as AMG 510 (35), might become a novel therapeutic target for LuM.

The HIPPO pathway is a cancer signaling network (36), and its alteration has been observed in approximately 10%

of MSS CRCs without *POLE* mutations (15). Here, the mutation or loss of copy numbers of tumor suppressor genes including *FAT1*, *FAT2*, *FAT3*, and *FAT4* in the HIPPO pathway were found in 33.3% of LuM, indicating that the HIPPO pathway might be activated and that a HIPPO pathway inhibitor might have a potential role in the treatment of LuM.

ICIs are not effective in 95% of patients with MSS mCRC (34), making it urgent to find new immunotherapies. Recently, durvalumab plus tremelimumab had better overall survival (OS) compared to placebo in MSS patients with a TMB >28 SNVs/Mb (21% of MSS patients) (37). Our results showed that patients with LuM were more likely to have higher TMB levels than patients with LiM, suggesting that patients with LuM may be a target population to receive combined ICIs. In the phase 1 trial REGONIVO, regorafenib plus nivolumab resulted in a 33% ORR in patients with MSS CRC (38). More recent data has shown that patients with LuM could receive more benefit from this treatment regimen than those with LiM in MSS CRC (39). These interesting findings might be explained partially by the relatively high TMB in LuM and the unexplored microenvironment in different metastatic organs. However, further analyses are required to find out if CRC patients with LuM could be the potential treatment population of ICIs.

This study has some limitations. First, the sample size was relatively small with minor statistical power due to the strict inclusion criteria, which allowed the close association of genetic differences with the metastatic phenotypes among different cohorts. Further studies with larger sample sizes in an independent cohort are essential to validate our findings. Second, most genetic differences were discovered as copy number alterations using NGS. These CNVs were not validated by RNA analysis or immunohistochemistry due to the lack of additional specimens. This is because the LuM and LiM specimens were collected prior to this study. Third, this pilot study showed the potential genetic differences and different amplification frequencies of certain genes between LuM and LiM, such as *ZFHX4* and *BRD4*. However, their detailed functions and affected pathways related to specific metastatic organs remain to be investigated, and our data are currently available only at the DNA level, with a lack of exploration at the RNA level and epigenetic level. Lastly, the results were obtained from left-sided MSS CRC, and could not be extrapolated to right-sided CRC. Right-sided CRC with LiM had a poorer prognosis compared to left-sided CRC (40), while those with LuM seemed to have similar survivals regardless of primary location (5). Therefore, the underlying genetic differences between LuM and LiM in right-sided CRC should be further investigated.

Conclusions

This study presented evidence that the genetic characteristics of LuM from left-sided MSS CRC were distinct from those of LiM from left-sided MSS CRC. Patients with LuM could be separated from those with LiM and without metastases based on CNV features of the primary tumors. *BRD4* and *HNF4A* inhibitors might reduce the risk of developing LuM. For LuM patients with MSS CRC, targeting the HIPPO pathway or *MET* alterations might become a novel approach, and ICIs combined with other agents need to be investigated, especially for patients with high TMB.

Acknowledgments

We thank American Journal Experts (https://www.aje.cn/) for linguistic assistance during the preparation of this manuscript.

Funding: This work was supported by the National Key Sci-Tech Special Project of China (grant number 2018ZX10302207).

Footnote

Reporting Checklist: The authors have completed the MDAR reporting checklist. Available at https://dx.doi.org/10.21037/atm-21-2221

Data Sharing Statement: Available at https://dx.doi.org/10.21037/atm-21-2221

Conflicts of Interest: All authors have completed the ICMJE uniform disclosure form (available at Available at https://dx.doi.org/10.21037/atm-21-2221). All authors report funding from the National Key Sci-Tech Special Project of China (grant number 2018ZX10302207). XZ, YC, JY, WY, BM, and HZ are from Genecast Biotechnology Co., Ltd. The authors have no other conflicts of interest to declare.

Ethics Statement: The authors are accountable for all aspects of the work in ensuring that questions related to the accuracy or integrity of any part of the work are appropriately investigated and resolved. This study was

conducted in accordance with the Declaration of Helsinki (as revised in 2013). This study was approved by the Beijing Cancer Hospital Ethics Committee (No. 2017KT91) and individual consent for this retrospective analysis was waived.

References

1. Siegel RL, Miller KD, Jemal A. Cancer statistics, 2018. CA Cancer J Clin 2018;68:7-30.
2. Qiu M, Yang D, Cosgrove D, et al. Pattern of distant metastases in colorectal cancer: a SEER based study. Oncotarget 2015;6:38658-66.
3. Li J, Yuan Y, Yang F, et al. Expert consensus on multidisciplinary therapy of colorectal cancer with lung metastases (2019 edition). J Hematol Oncol 2019;12:16.
4. Tampellini M, Ottone A, Bellini E, et al. The role of lung metastasis resection in improving outcome of colorectal cancer patients: results from a large retrospective study. Oncologist 2012;17:1430-8.
5. Wang Z, Wang X, Yuan J, et al. Survival Benefit of Palliative Local Treatments and Efficacy of Different Pharmacotherapies in Colorectal Cancer With Lung Metastasis: Results From a Large Retrospective Study. Clin Colorectal Cancer 2018;17:e233-55.
6. Imanishi M, Yamamoto Y, Hamano Y, et al. Efficacy of adjuvant chemotherapy after resection of pulmonary metastasis from colorectal cancer: a propensity score-matched analysis. Eur J Cancer 2019;106:69-77.
7. Li WH. Oncological outcome of unresectable lung metastases without extrapulmonary metastases in colorectal cancer. World J Gastroenterol 2010;16:3318.
8. Nozawa H, Ishihara S, Kawai K, et al. Characterization of Conversion Chemotherapy for Secondary Surgical Resection in Colorectal Cancer Patients with Lung Metastases. Oncology 2017;92:135-41.
9. Prasanna T, Craft PS, Chua YJ, et al. The outcome of patients (pts) with metastatic colorectal cancer (mCRC) based on site of metastases (mets) and the impact of molecular markers and site of primary cancer on metastatic pattern. J Clin Oncol 2017;35:abstr 3560.
10. El-Deiry WS, Vijayvergia N, Xiu J, et al. Molecular profiling of 6,892 colorectal cancer samples suggests different possible treatment options specific to metastatic sites. Cancer Biol Ther 2015;16:1726-37.
11. Sartore-Bianchi A, Trusolino L, Martino C, et al. Dual-targeted therapy with trastuzumab and lapatinib in treatment-refractory, KRAS codon 12/13 wild-type, HER2-positive metastatic colorectal cancer (HERACLES): a proof-of-concept, multicentre, open-label, phase 2 trial. Lancet Oncol 2016;17:738-46.
12. Hainsworth JD, Meric-Bernstam F, Swanton C, et al. Targeted Therapy for Advanced Solid Tumors on the Basis of Molecular Profiles: Results From MyPathway, an Open-Label, Phase IIa Multiple Basket Study. J Clin Oncol 2018;36:536-42.
13. Kovaleva V, Geissler AL, Lutz L, et al. Spatio-temporal mutation profiles of case-matched colorectal carcinomas and their metastases reveal unique de novo mutations in metachronous lung metastases by targeted next generation sequencing. Mol Cancer 2016;15:63.
14. Hou J, Zhang Y, Zhu Z. Gene heterogeneity in metastasis of colorectal cancer to the lung. Semin Cell Dev Biol 2017;64:58-64.
15. Sanchez-Vega F, Mina M, Armenia J, et al. Oncogenic Signaling Pathways in The Cancer Genome Atlas. Cell 2018;173:321-37.e10.
16. Chiang JM, Hsieh PS, Chen JS, et al. Rectal cancer level significantly affects rates and patterns of distant metastases among rectal cancer patients post curative-intent surgery without neoadjuvant therapy. World J Surg Oncol 2014;12:197.
17. He WZ, Hu WM, Wang F, et al. Comparison of Mismatch Repair Status Between Primary and Matched Metastatic Sites in Patients With Colorectal Cancer. J Natl Compr Canc Netw 2019;17:1174-83.
18. Cejas P, López-Gómez M, Aguayo C, et al. KRAS mutations in primary colorectal cancer tumors and related metastases: a potential role in prediction of lung metastasis. PLoS One 2009;4:e8199.
19. Kim MJ, Lee H, Kim JH, et al. Different metastatic pattern according to the KRAS mutational status and site-specific discordance of KRAS status in patients with colorectal cancer. BMC Cancer 2012;12:347.
20. Kemeny NE, Chou JF, Capanu M, et al. KRAS mutation influences recurrence patterns in patients undergoing hepatic resection of colorectal metastases. Cancer

2014;120:3965-71.
21. Morris VK, Lucas FA, Overman MJ, et al. Clinicopathologic characteristics and gene expression analyses of non-KRAS 12/13, RAS-mutated metastatic colorectal cancer. Ann Oncol 2014;25:2008-14.
22. Russo AL, Borger DR, Szymonifka J, et al. Mutational analysis and clinical correlation of metastatic colorectal cancer. Cancer 2014;120:1482-90.
23. Casimiro S, Fernandes A, Oliveira AG, et al. Metadherin expression and lung relapse in patients with colorectal carcinoma. Clin Exp Metastasis 2014;31:689-96.
24. Chudnovsky Y, Kim D, Zheng S, et al. ZFHX4 interacts with the NuRD core member CHD4 and regulates the glioblastoma tumor-initiating cell state. Cell Rep 2014;6:313-24.
25. Xu C. Exploring genetic mechanism of ZHFX4 in colorectal cancer by genome analysis. Shenyang: Dalian Medical University, 2016.
26. Xu K, Wang J, Gao J, et al. GATA binding protein 2 overexpression is associated with poor prognosis in KRAS mutant colorectal cancer. Oncol Rep 2016;36:1672-8.
27. Lao VV, Welcsh P, Luo Y, et al. Altered RECQ Helicase Expression in Sporadic Primary Colorectal Cancers. Transl Oncol 2013;6:458-69.
28. Liu Z, Wang P, Chen H, et al. Drug Discovery Targeting Bromodomain-Containing Protein 4. J Med Chem 2017;60:4533-58.
29. Hu Y, Zhou J, Ye F, et al. BRD4 inhibitor inhibits colorectal cancer growth and metastasis. Int J Mol Sci 2015;16:1928-48.
30. Xu C, Ooi WF, Qamra A, et al. HNF4α pathway mapping identifies wild-type IDH1 as a targetable metabolic node in gastric cancer. Gut 2020;69:231-42.
31. Schwartz B, Algamas-Dimantov A, Hertz R, et al. Inhibition of colorectal cancer by targeting hepatocyte nuclear factor-4alpha. Int J Cancer 2009;124:1081-9.
32. Rimassa L, Bozzarelli S, Pietrantonio F, et al. Phase II Study of Tivantinib and Cetuximab in Patients With KRAS Wild-type Metastatic Colorectal Cancer With Acquired Resistance to EGFR Inhibitors and Emergence of MET Overexpression: Lesson Learned for Future Trials With EGFR/MET Dual Inhibition. Clin Colorectal Cancer 2019;18:125-32.e2.
33. Bardelli A, Corso S, Bertotti A, et al. Amplification of the MET receptor drives resistance to anti-EGFR therapies in colorectal cancer. Cancer Discov 2013;3:658-73.
34. Yaeger R, Chatila WK, Lipsyc MD, et al. Clinical Sequencing Defines the Genomic Landscape of Metastatic Colorectal Cancer. Cancer Cell 2018;33:125-36.
35. Govindan R, Fakih MG, Price TJ, et al. 446PD - Phase I study of AMG 510, a novel molecule targeting KRAS G12C mutant solid tumours. Ann Oncol 2019;30:v163-4.
36. Harvey KF, Zhang X, Thomas DM. The Hippo pathway and human cancer. Nat Rev Cancer 2013;13:246-57.
37. Chen EX, Jonker DJ, Loree JM, et al. CCTG CO.26: Updated analysis and impact of plasma-detected microsatellite stability (MSS) and tumor mutation burden (TMB) in a phase II trial of durvalumab (D) plus tremelimumab (T) and best supportive care (BSC) versus BSC alone in patients (pts) with refractory metastatic colorectal carcinoma (rmCRC). J Clin Oncol 2019;37:abstr 3512.
38. Fukuoka S, Hara H, Takahashi N, et al. Regorafenib plus nivolumab in patients with advanced gastric (GC) or colorectal cancer (CRC): An open-label, dose-finding, and dose-expansion phase 1b trial (REGONIVO, EPOC1603). J Clin Oncol 2020;38:2053-61.
39. Shitara K, Hara H, Takahashi N, et al. Updated results from a phase Ib trial of regorafenib plus nivolumab in patients with advanced colorectal or gastric cancer (REGONIVO, EPOC1603). J Clin Oncol 2020;38:abstr135.
40. Tang W, Ren L, Liu T, et al. Bevacizumab Plus mFOLFOX6 Versus mFOLFOX6 Alone as First-Line Treatment for RAS Mutant Unresectable Colorectal Liver-Limited Metastases: The BECOME Randomized Controlled Trial. J Clin Oncol 2020;38:3175-84.

(English Language Editor: C. Betlazar-Maseh)

Cite this article as: Wang Z, Zheng X, Wang X, Chen Y, Li Z, Yu J, Yang W, Mao B, Zhang H, Li J, Shen L. Genetic differences between lung metastases and liver metastases from left-sided microsatellite stable colorectal cancer: next generation sequencing and clinical implications. Ann Transl Med 2021;9(12):967. doi: 10.21037/atm-21-2221

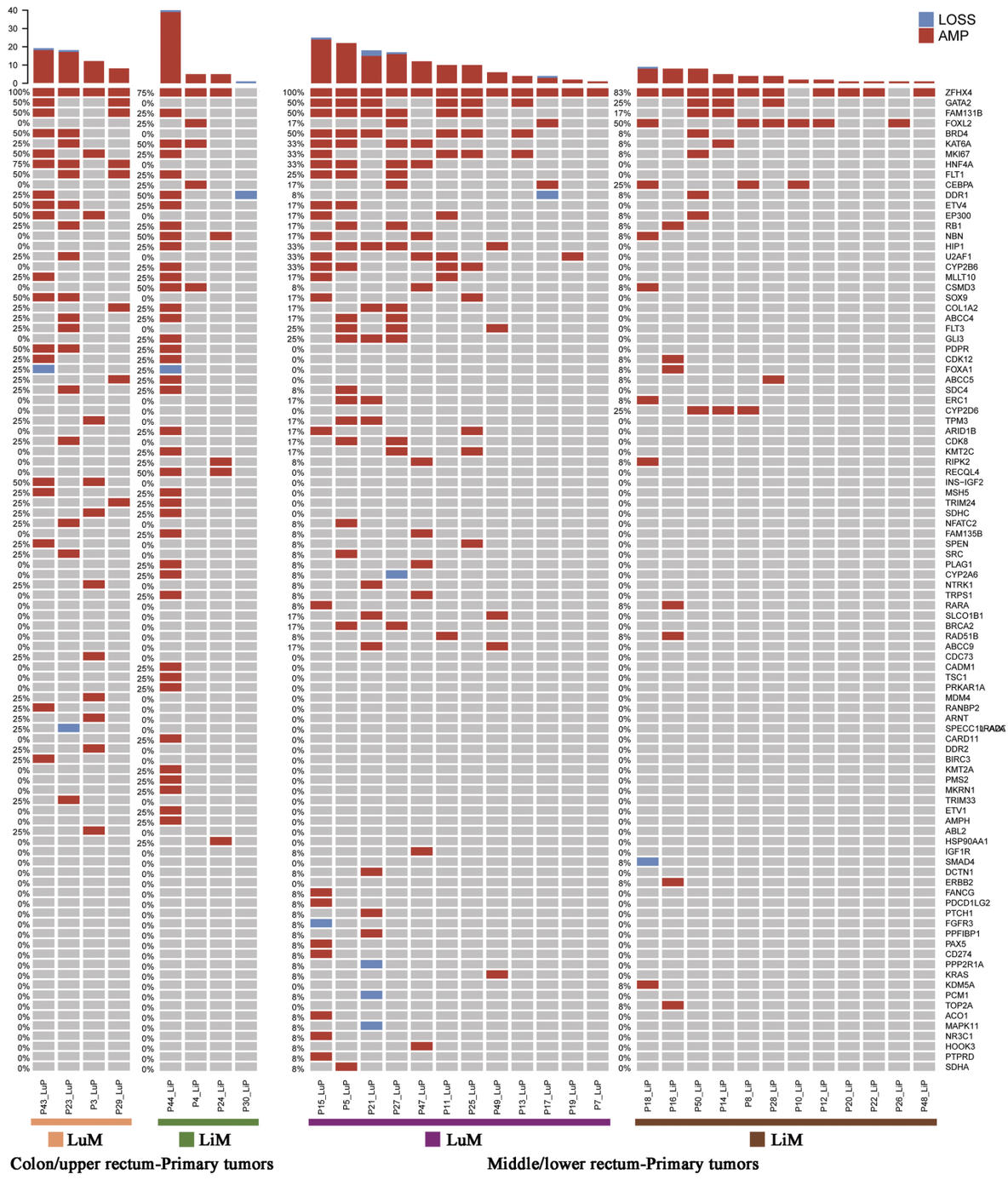

Figure S1 Copy number alterations at different locations in the primary tumors from the LuM and LiM cohorts. LuM, lung metastases; LiM, liver metastases; AMP, amplification.

https://dx.doi.org/10.21037/atm-21-2221

Table S1 Single nucleotide variations in the primary tumors from the LuM, LiM and control cohorts, n (%)

Gene	LuM + LiM	Control	P	LuM	LiM	P
	n=32	n=10		n=16	n=16	
TP53	20 (62.5)	9 (90.0)	0.211	11 (68.8)	9 (56.3)	0.716
APC	17 (53.1)	8 (80.0)	0.253	9 (56.3)	10 (62.5)	1.000
KRAS	8 (25.0)	2 (20.0)	1.000	6 (37.5)	5 (31.3)	1.000
FBXW7	5 (15.6)	2 (20.0)	1.000	3 (18.8)	2 (12.5)	1.000
PIK3CA	5 (15.6)	1 (10.0)	1.000	4 (25.0)	0 (0.0)	0.101
ALK	3 (9.4)	0 (0.0)	1.000	3 (18.8)	2 (12.5)	1.000
ERBB2	3 (9.4)	0 (0.0)	1.000	3 (18.8)	1 (6.3)	0.600
ERBB3	4 (12.5)	1 (10.0)	1.000	3 (18.8)	0 (0.0)	0.226
RYR2	3 (9.4)	0 (0.0)	1.000	3 (18.8)	1 (6.3)	0.600
IDH1	1 (3.1)	0 (0.0)	1.000	1 (6.3)	2 (12.5)	1.000
HRAS	2 (6.3)	1 (10.0)	1.000	1 (6.3)	1 (6.3)	1.000
TSPYL2	3 (9.4)	0 (0.0)	1.000	3 (18.8)	0 (0.0)	0.226
DST	2 (6.3)	1 (10.0)	1.000	1 (6.3)	1 (6.3)	1.000
GNAS	3 (9.4)	0 (0.0)	1.000	3 (18.8)	0 (0.0)	0.226
SMAD4	3 (9.4)	2 (20.0)	0.729	1 (6.3)	0 (0.0)	1.000
NTRK1	0 (0.0)	0 (0.0)	–	0 (0.0)	3 (18.8)	0.226
LGALS3	3 (9.4)	0 (0.0)	1.000	3 (18.8)	0 (0.0)	0.226
EGFR	2 (6.3)	0 (0.0)	1.000	2 (12.5)	1 (6.3)	1.000
BRD7	2 (6.3)	0 (0.0)	1.000	2 (12.5)	1 (6.3)	1.000
EIF3A	3 (9.4)	0 (0.0)	1.000	3 (18.8)	0 (0.0)	0.226
AMER1	2 (6.3)	1 (10.0)	1.000	1 (6.3)	1 (6.3)	1.000
RNF43	2 (6.3)	0 (0.0)	1.000	2 (12.5)	1 (6.3)	1.000
MEF2B	1 (3.1)	0 (0.0)	1.000	1 (6.3)	2 (12.5)	1.000
TET2	2 (6.3)	0 (0.0)	1.000	2 (12.5)	1 (6.3)	1.000
NRAS	2 (6.3)	1 (10.0)	1.000	1 (6.3)	1 (6.3)	1.000
PRKCB	2 (6.3)	0 (0.0)	1.000	2 (12.5)	1 (6.3)	1.000
PFKFB1	3 (9.4)	0 (0.0)	1.000	3 (18.8)	0 (0.0)	0.226

LuM, lung metastases; LiM, liver metastases.

https://dx.doi.org/10.21037/atm-21-2221

Table S2 Copy number variations in the primary tumors from the LuM, LiM and control cohorts, n (%)

Gene	LuM + LiM (n=32)	Control (n=10)	P	LuM (n=16)	LiM (n=16)	P
ZFHX4	29 (90.6)	1 (10.0)	<0.001[#]	16 (100.0)	13 (81.3)	0.226
GATA2	11 (34.4)	0 (0.0)	0.081	8 (50.0)	3 (18.8)	0.135
FAM131B	11 (34.4)	0 (0.0)	0.081	8 (50.0)	3 (18.8)	0.135
HNF4A	7 (21.9)	4 (40.0)	0.468	7 (43.8)	0 (0.0)	0.007[#]
RECQL4	2 (6.3)	7 (70.0)	<0.001[#]	0 (0.0)	2 (12.5)	0.484
FOXL2	9 (28.1)	0 (0.0)	0.147	2 (12.5)	7 (43.8)	0.113
BRD4	9 (28.1)	0 (0.0)	0.147	8 (50.0)	1 (6.3)	0.015[#]
CEBPA	6 (18.8)	3 (30.0)	0.753	2 (12.5)	4 (25.0)	0.654
KAT6A	8 (25.0)	0 (0.0)	0.195	5 (31.3)	3 (18.8)	0.685
MKI67	8 (25.0)	0 (0.0)	0.195	6 (37.5)	2 (12.5)	0.220
FLT1	6 (18.8)	2 (20.0)	1.000	5 (31.3)	1 (6.3)	0.172
DDR1 *	5 (15.6)	2 (20.0)	1.000	2 (12.5)	3 (18.8)	1.000
NBN	5 (15.6)	2 (20.0)	1.000	2 (12.5)	3 (18.8)	1.000
RIPK2	3 (9.4)	3 (30.0)	0.267	1 (6.3)	2 (12.5)	1.000
RB1	5 (15.6)	1 (10.0)	1.000	3 (18.8)	2 (12.5)	1.000
CYP2A6 *	2 (6.3)	3 (30.0)	0.143	1 (6.3)	1 (6.3)	1.000
HIP1	5 (15.6)	0 (0.0)	0.440	4 (25.0)	1 (6.3)	0.333
U2AF1	5 (15.6)	0 (0.0)	0.440	5 (31.3)	0 (0.0)	0.043[#]
EP300	5 (15.6)	0 (0.0)	0.440	4 (25.0)	1 (6.3)	0.333
ETV4	5 (15.6)	0 (0.0)	0.440	4 (25.0)	1 (6.3)	0.333
CYP2B6	5 (15.6)	0 (0.0)	0.440	4 (25.0)	1 (6.3)	0.333
CDK8	3 (9.4)	2 (20.0)	0.729	3 (18.8)	0 (0.0)	0.226
SDC4	3 (9.4)	2 (20.0)	0.729	2 (12.5)	1 (6.3)	1.000
CSMD3	4 (12.5)	1 (10.0)	1.000	1 (6.3)	3 (18.8)	0.600
ABCC4	4 (12.5)	1 (10.0)	1.000	3 (18.8)	1 (6.3)	0.600
GLI3	4 (12.5)	1 (10.0)	1.000	3 (18.8)	1 (6.3)	0.600
NFATC2	2 (6.3)	2 (20.0)	0.236	2 (12.5)	0 (0.0)	0.484
SRC	2 (6.3)	2 (20.0)	0.236	2 (12.5)	0 (0.0)	0.484
TRPS1	2 (6.3)	2 (20.0)	0.236	1 (6.3)	1 (6.3)	1.000
MLLT10	4 (12.5)	0 (0.0)	0.557	3 (18.8)	1 (6.3)	0.600
FLT3	4 (12.5)	0 (0.0)	0.557	4 (25.0)	0 (0.0)	0.101
SOX9	4 (12.5)	0 (0.0)	0.557	4 (25.0)	0 (0.0)	0.101
COL1A2	4 (12.5)	0 (0.0)	0.557	3 (18.8)	1 (6.3)	0.600
CYP2D6	3 (9.4)	1 (10.0)	1.000	0 (0.0)	3 (18.8)	0.226
PDPR	3 (9.4)	1 (10.0)	1.000	2 (12.5)	1 (6.3)	1.000
FLCN[&]	0 (0.0)	3 (30.0)	0.010[#]	0 (0.0)	0 (0.0)	/
ETV1	1 (3.1)	2 (20.0)	0.136	0 (0.0)	1 (6.3)	1.000
TPM3	3 (9.4)	0 (0.0)	1.000	3 (18.8)	0 (0.0)	0.226
ERC1	3 (9.4)	0 (0.0)	1.000	2 (12.5)	1 (6.3)	1.000
CDK12	3 (9.4)	0 (0.0)	1.000	1 (6.3)	2 (12.5)	1.000
ARID1B	3 (9.4)	0 (0.0)	1.000	2 (12.5)	1 (6.3)	1.000
*FOXA1**	3 (9.4)	0 (0.0)	1.000	1 (6.3)	2 (12.5)	1.000
FAM135B	2 (6.3)	1 (10.0)	1.000	1 (6.3)	1 (6.3)	1.000
BRCA2	2 (6.3)	1 (10.0)	1.000	2 (12.5)	0 (0.0)	0.484
PLAG1	2 (6.3)	1 (10.0)	1.000	1 (6.3)	1 (6.3)	1.000
KMT2C	3 (9.4)	0 (0.0)	1.000	2 (12.5)	1 (6.3)	1.000
ABCC5	3 (9.4)	0 (0.0)	1.000	1 (6.3)	2 (12.5)	1.000

*, CNVs included both loss and amplification; [&], only the FLCN gene showed a loss of copy number. Other genes showed only amplification; [#], P values <0.05. LuM, lung metastases; LiM, liver metastases.

https://dx.doi.org/10.21037/atm-21-2221

Table S3 Alteration frequencies of colorectal cancer pathways and related genes in the primary tumors and metastatic lesions

Pathway	Gene	Primary tumors, n (%)					Metastatic lesions, n (%)		
		LuM cohort (n=16)	LiM cohort (n=16)	Control cohort (n=10)	$P_{LuM\ vs.\ LiM}$	$P_{LuM\ vs.\ Control}$	LuM cohort (n=15)	LiM cohort (n=18)	P
WNT		10 (62.5)	11 (68.8)	8 (80.0)	1.000	0.420	9 (60.0)	13 (72.2)	0.488
	APC	9 (56.3)	10 (62.5)	8 (80.0)	1.000	0.399	8 (53.3)	12 (66.7)	0.493
	AMER1	1 (6.3)	1 (6.3)	1 (10.0)	1.000	1.000	0 (0.0)	1 (5.6)	1.000
	RNF43	2 (12.5)	1 (6.3)	0 (0.0)	1.000	0.508	1 (6.7)	0 (0.0)	0.455
	CTNNB1	1 (6.3)	0 (0.0)	0 (0.0)	1.000	1.000	1 (6.7)	0 (0.0)	0.455
	GSK3B	0 (0.0)	0 (0.0)	0 (0.0)	–	–	1 (6.7)	1 (5.6)	1.000
	SFRP2	0 (0.0)	0 (0.0)	0 (0.0)	–	–	0 (0.0)	1 (5.6)	1.000
	TCF7L2	0 (0.0)	0 (0.0)	1 (10.0)	–	0.385	0 (0.0)	0 (0.0)	–
TGFβ		2 (12.5)	3 (18.8)	3 (30.0)	1.000	0.340	4 (26.7)	4 (22.2)	1.000
	SMAD4	1 (6.3)	1 (6.3)	2 (20.0)	1.000	0.538	3 (20.0)	1 (5.6)	0.308
	SMAD2	0 (0.0)	0 (0.0)	1 (10.0)	–	0.385	1 (6.7)	2 (11.1)	1.000
	SMAD3	1 (6.3)	1 (6.3)	0 (0.0)	1.000	1.000	0 (0.0)	0 (0.0)	–
	TGFBR1	0 (0.0)	0 (0.0)	0 (0.0)	–	–	0 (0.0)	2 (11.1)	0.489
	ACVR1B	0 (0.0)	0 (0.0)	0 (0.0)	–	–	1 (6.7)	0 (0.0)	0.455
	TGFBR2	0 (0.0)	1 (6.3)	0 (0.0)	1.000	–	0 (0.0)	0 (0.0)	–
RTK/RAS		14 (87.5)	11 (68.8)	7 (70.0)	0.394	0.340	15 (100.0)	13 (72.2)	0.049#
	KRAS	7 (43.8)	5 (31.3)	3 (30.0)	0.716	0.683	11 (73.3)	7 (38.9)	0.080
	EGFR	2 (12.5)	1 (6.3)	1 (10.0)	1.000	1.000	1 (6.7)	4 (22.2)	0.346
	ERBB3	3 (18.8)	0 (0.0)	1 (10.0)	0.226	1.000	2 (13.3)	3 (16.7)	1.000
	NTRK1	2 (12.5)	3 (18.8)	0 (0.0)	1.000	0.508	2 (13.3)	2 (11.1)	1.000
	HRAS	1 (6.3)	1 (6.3)	2 (20.0)	1.000	0.538	3 (20.0)	1 (5.6)	0.308
	ALK	3 (18.8)	2 (12.5)	0 (0.0)	1.000	0.262	0 (0.0)	2 (11.1)	0.489
	MET	0 (0.0)	0 (0.0)	0 (0.0)	–	–	6 (40.0)	1 (5.6)	0.030#
	ERBB2	3 (18.8)	1 (6.3)	0 (0.0)	0.600	0.262	1 (6.7)	1 (5.6)	1.000
	FLT3	4 (25.0)	0 (0.0)	0 (0.0)	0.101	0.136	0 (0.0)	2 (11.1)	0.489
	KIT	2 (12.5)	0 (0.0)	0 (0.0)	0.484	0.508	2 (13.3)	2 (11.1)	1.000
	NRAS	1 (6.3)	1 (6.3)	1 (10.0)	1.000	1.000	1 (6.7)	1 (5.6)	1.000
	FGFR3	2 (12.5)	0 (0.0)	0 (0.0)	0.484	0.508	1 (6.7)	1 (5.6)	1.000
	BRAF	1 (6.3)	0 (0.0)	0 (0.0)	1.000	1.000	1 (6.7)	1 (5.6)	1.000
	ERBB4	1 (6.3)	0 (0.0)	1 (10.0)	1.000	1.000	0 (0.0)	1 (5.6)	1.000
	FGFR2	0 (0.0)	0 (0.0)	0 (0.0)	–	–	1 (6.7)	2 (11.1)	1.000
	MAP2K1	2 (12.5)	0 (0.0)	0 (0.0)	0.484	0.508	1 (6.7)	0 (0.0)	0.455
	NTRK3	1 (6.3)	0 (0.0)	1 (10.0)	1.000	1.000	1 (6.7)	0 (0.0)	0.455
	PDGFRA	2 (12.5)	0 (0.0)	0 (0.0)	0.484	0.508	1 (6.7)	0 (0.0)	0.455
	CBL	0 (0.0)	0 (0.0)	0 (0.0)	–	–	1 (6.7)	1 (5.6)	1.000
	NF1	0 (0.0)	0 (0.0)	0 (0.0)	–	–	2 (13.3)	0 (0.0)	0.199
	PTPN11	0 (0.0)	0 (0.0)	0 (0.0)	–	–	1 (6.7)	1 (5.6)	1.000
	RET	1 (6.3)	0 (0.0)	0 (0.0)	1.000	1.000	1 (6.7)	0 (0.0)	0.455
	ARAF	0 (0.0)	0 (0.0)	0 (0.0)	–	–	1 (6.7)	0 (0.0)	0.455
	FGFR1	0 (0.0)	0 (0.0)	0 (0.0)	–	–	0 (0.0)	1 (5.6)	1.000
	FGFR4	1 (6.3)	0 (0.0)	0 (0.0)	1.000	1.000	0 (0.0)	0 (0.0)	–
	IGF1R	1 (6.3)	0 (0.0)	0 (0.0)	1.000	1.000	0 (0.0)	0 (0.0)	–
	MAP2K2	0 (0.0)	0 (0.0)	0 (0.0)	–	–	1 (6.7)	0 (0.0)	0.455
	MAPK1	1 (6.3)	0 (0.0)	0 (0.0)	1.000	1.000	0 (0.0)	0 (0.0)	–
	ROS1	0 (0.0)	0 (0.0)	1 (10.0)	–	0.385	0 (0.0)	0 (0.0)	–
PI3K		8 (50.0)	4 (25.0)	2 (20.0)	0.273	0.218	8 (53.3)	7 (38.9)	0.494
	PIK3CA	4 (25.0)	0 (0.0)	1 (10.0)	0.101	0.617	1 (6.7)	3 (16.7)	0.607
	MTOR	2 (12.5)	0 (0.0)	0 (0.0)	0.484	0.508	0 (0.0)	3 (16.7)	0.233

Table S3 (*continued*)

https://dx.doi.org/10.21037/atm-21-2221

Table S3 (*continued*)

Pathway	Gene	Primary tumors, n (%)					Metastatic lesions, n (%)		
		LuM cohort (n=16)	LiM cohort (n=16)	Control cohort (n=10)	$P_{LuM\ vs.\ LiM}$	$P_{LuM\ vs.\ Control}$	LuM cohort (n=15)	LiM cohort (n=18)	P
	STK11	1 (6.3)	0 (0.0)	1 (10.0)	1.000	1.000	2 (13.3)	0 (0.0)	0.199
	TSC1	0 (0.0)	1 (6.3)	0 (0.0)	1.000	–	1 (6.7)	2 (11.1)	1.000
	PPP2R1A	1 (6.3)	0 (0.0)	0 (0.0)	1.000	1.000	2 (13.3)	0 (0.0)	0.199
	PTEN	1 (6.3)	1 (6.3)	0 (0.0)	1.000	1.000	0 (0.0)	1 (5.6)	1.000
	AKT1	0 (0.0)	0 (0.0)	0 (0.0)	–	–	2 (13.3)	0 (0.0)	0.199
	AKT3	2 (12.5)	0 (0.0)	0 (0.0)	0.484	0.508	0 (0.0)	0 (0.0)	–
	PIK3CB	1 (6.3)	0 (0.0)	0 (0.0)	1.000	1.000	1 (6.7)	0 (0.0)	0.455
	PIK3R1	0 (0.0)	1 (6.3)	0 (0.0)	1.000	–	0 (0.0)	1 (5.6)	1.000
	TSC2	1 (6.3)	0 (0.0)	0 (0.0)	1.000	1.000	1 (6.7)	0 (0.0)	0.455
	PIK3R2	0 (0.0)	0 (0.0)	0 (0.0)	–	–	1 (6.7)	0 (0.0)	0.455
	RICTOR	0 (0.0)	1 (6.3)	0 (0.0)	1.000	–	0 (0.0)	0 (0.0)	–
P53		12 (75.0)	10 (62.5)	9 (90.0)	0.704	0.617	14 (93.3)	12 (66.7)	0.095
	TP53	11 (68.8)	9 (56.3)	9 (90.0)	0.716	0.352	13 (86.7)	12 (66.7)	0.242
	MDM4	2 (12.5)	0 (0.0)	0 (0.0)	0.484	0.508	2 (13.3)	0 (0.0)	0.199
	ATM	0 (0.0)	0 (0.0)	0 (0.0)	–	–	1 (6.7)	0 (0.0)	0.455
	RPS6KA3	0 (0.0)	1 (6.3)	0 (0.0)	1.000	–	0 (0.0)	0 (0.0)	–
NRF2		1 (6.3)	1 (6.3)	0 (0.0)	1.000	1.000	0 (0.0)	0 (0.0)	–
	CUL3	0 (0.0)	1 (6.3)	0 (0.0)	1.000	–	0 (0.0)	0 (0.0)	–
	KEAP1	1 (6.3)	0 (0.0)	0 (0.0)	1.000	1.000	0 (0.0)	0 (0.0)	–
NOTCH		9 (56.3)	6 (37.5)	3 (30.0)	0.479	0.248	7 (46.7)	8 (44.4)	1.000
	FBXW7	3 (18.8)	2 (12.5)	2 (20.0)	1.000	1.000	2 (13.3)	3 (16.7)	1.000
	EP300	4 (25.0)	1 (6.3)	0 (0.0)	0.333	0.136	2 (13.3)	2 (11.1)	1.000
	KDM5A	0 (0.0)	1 (6.3)	0 (0.0)	1.000	–	3 (20.0)	3 (16.7)	1.000
	NOTCH1	1 (6.3)	1 (6.3)	1 (10.0)	1.000	1.000	2 (13.3)	0 (0.0)	0.199
	NOTCH2	1 (6.3)	0 (0.0)	0 (0.0)	1.000	1.000	1 (6.7)	2 (11.1)	1.000
	NOTCH3	1 (6.3)	1 (6.3)	0 (0.0)	1.000	1.000	0 (0.0)	0 (0.0)	–
	SPEN	2 (12.5)	0 (0.0)	0 (0.0)	0.484	0.508	0 (0.0)	0 (0.0)	–
	NCOR1	1 (6.3)	0 (0.0)	0 (0.0)	1.000	1.000	0 (0.0)	0 (0.0)	–
MYC		1 (6.3)	0 (0.0)	0 (0.0)	1.000	1.000	2 (13.3)	0 (0.0)	0.199
	MAX	0 (0.0)	0 (0.0)	0 (0.0)	–	–	1 (6.7)	0 (0.0)	0.455
	MYCL	1 (6.3)	0 (0.0)	0 (0.0)	1.000	1.000	0 (0.0)	0 (0.0)	–
	MYCN	0 (0.0)	0 (0.0)	0 (0.0)	–	–	1 (6.7)	0 (0.0)	0.455
HIPPO		2 (12.5)	2 (12.5)	0 (0.0)	1.000	0.508	5 (33.3)	1 (5.6)	0.070
	FAT3	0 (0.0)	1 (6.3)	0 (0.0)	1.000	–	3 (20.0)	0 (0.0)	0.083
	FAT4	0 (0.0)	0 (0.0)	0 (0.0)	–	–	2 (13.3)	1 (5.6)	0.579
	FAT1	0 (0.0)	0 (0.0)	0 (0.0)	–	–	1 (6.7)	1 (5.6)	1.000
	FAT2	1 (6.3)	1 (6.3)	0 (0.0)	1.000	1.000	0 (0.0)	0 (0.0)	–
	NF2	1 (6.3)	0 (0.0)	0 (0.0)	1.000	1.000	0 (0.0)	0 (0.0)	–
Cell cycle		5 (31.3)	3 (18.8)	2 (20.0)	0.685	0.668	4 (26.7)	5 (27.8)	1.000
	RB1	4 (25.0)	3 (18.8)	1 (10.0)	1.000	0.617	2 (13.3)	3 (16.7)	1.000
	CDK4	0 (0.0)	0 (0.0)	1 (10.0)	–	0.385	2 (13.3)	0 (0.0)	0.199
	CCND3	0 (0.0)	0 (0.0)	0 (0.0)	–	–	0 (0.0)	1 (5.6)	1.000
	CCNE1	0 (0.0)	0 (0.0)	0 (0.0)	–	–	1 (6.7)	0 (0.0)	0.455
	CDKN1A	0 (0.0)	0 (0.0)	0 (0.0)	–	–	1 (6.7)	0 (0.0)	0.455
	CDKN2C	0 (0.0)	0 (0.0)	0 (0.0)	–	–	1 (6.7)	0 (0.0)	0.455
	E2F1	1 (6.3)	0 (0.0)	0 (0.0)	1.000	1.000	0 (0.0)	0 (0.0)	–
	CDKN2A	0 (0.0)	0 (0.0)	0 (0.0)	–	–	0 (0.0)	1 (5.6)	1.000

[#] P values <0.05. LuM, lung metastases; LiM, liver metastases.

https://dx.doi.org/10.21037/atm-21-2221

Table S4 Comparison of the frequencies of possible gene alterations associated with immune checkpoint inhibitors

Gene alteration	Cohort (n)					P					
	LuM-P (n=16)	LiM-P (n=16)	Control-P (n=10)	LuM-M (n=15)	LiM-M (n=18)	LuM-P *vs.* LiM-P	LuM-P *vs.* Control-P	LiM-P *vs.* Control-P	LuM-M *vs.* LiM-M	LuM-P *vs.* LuM-M	LiM-P *vs.* LiM-M
TP53											
Mutation											
+	11	9	9	13	12	0.716	0.352	0.099	0.242	0.394	0.725
–	5	7	1	2	6						
KRAS											
Mutation											
+	6	5	2	9	7	1	0.42	0.668	0.303	0.289	0.729
–	10	11	8	6	11						
NRAS											
Mutation											
+	1	1	1	1	1	1	1	1	1	1	1
–	15	15	9	14	17						
ERCC2											
Mutation											
+	0	2	0	3	0	0.484	–	0.508	0.083	0.101	0.214
–	16	14	10	12	18						
POLE											
Loss											
+	0	0	1	0	0	–	0.385	0.385	–	–	–
–	16	16	9	15	18						
Mutation											
+	1	1	0	1	0	1	1	1	0.455	1	0.471
–	15	15	10	14	18						
MLH1											
Mutation											
+	1	1	0	1	1	1	1	1	1	1	1
–	15	15	10	14	17						
PMS2											
Mutation											
+	2	0	0	1	0	0.484	0.508	–	0.455	1	–
–	14	16	10	14	18						
MSH6											
Mutation											
+	2	0	0	0	0	0.484	0.508	–	–	0.484	–
–	14	16	10	15	18						
BRCA2											
Mutation											
+	0	0	0	1	1	–	–	–	1	1	1
–	16	16	10	14	17						
MDM4											
Gain											
+	1	0	0	1	0	1	1	–	0.455	1	–
–	15	16	10	14	18						
PBRM1											
Mutation											
+	1	0	0	0	0	1	1	–	–	1	–
–	15	16	10	15	18						

Table S4 (*continued*)

https://dx.doi.org/10.21037/atm-21-2221

Table S4 (*continued*)

Gene alteration	Cohort (n)					P					
	LuM-P (n=16)	LiM-P (n=16)	Control-P (n=10)	LuM-M (n=15)	LiM-M (n=18)	LuM-P *vs.* LiM-P	LuM-P *vs.* Control-P	LiM-P *vs.* Control-P	LuM-M *vs.* LiM-M	LuM-P *vs.* LuM-M	LiM-P *vs.* LiM-M
BRCA1											
Mutation											
+	0	0	0	0	1	–	–	–	1	–	1
–	16	16	10	15	17						
ATM											
Mutation											
+	0	0	0	1	0	–	–	–	0.455	1	–
–	16	16	10	14	18						
EGFR											
Gain											
+	0	0	1	1	1	–	0.385	0.385	1	0.484	1
–	16	16	9	14	17						
Mutation											
+	2	1	0	0	3	1	0.508	1	0.233	0.484	0.604
–	14	15	10	15	15						
STK11											
Mutation											
+	1	0	0	2	0	1	1	–	0.199	0.6	–
–	15	16	10	13	18						
MET											
Mutation											
+	0	0	0	2	1	–	–	–	0.579	0.226	1
–	16	16	10	13	17						
CTNNB1											
Mutation											
+	1	0	0	1	0	1	1	–	0.455	1	–
–	15	16	10	14	18						
JAK1											
Mutation											
+	0	0	0	1	0	–	–	–	0.455	1	–
–	16	16	10	14	18						
PTEN											
Loss											
+	0	0	0	0	1	–	–	–	1	–	1
–	16	16	10	15	17						

LuM, lung metastases; LiM, liver metastases; P, primary tumor; M, metastatic lesion.

https://dx.doi.org/10.21037/atm-21-2221